Nonharmonic phonons in MgB_{2} at elevated temperatures

N. D. Markovskiy, J. A. Muñoz, M. S. Lucas, Chen W. Li, O. Delaire, M. B. Stone, D. L. Abernathy, and B. Fultz

Phys. Rev. B **83**, 174301 — Published 4 May 2011

DOI: 10.1103/PhysRevB.83.174301

Non-harmonic phonons in MgB_2 at elevated temperatures

N. D. Markovskiy[1], J. A. Muñoz[1], M. S. Lucas[2], Chen W. Li[1], O. Delaire[2], M. B. Stone[2], D. L. Abernathy[2] and B. Fultz[1]
[1] *California Institute of Technology, Department of Applied Physics and Materials Science, Pasadena, California 91125, USA*
[2] *Oak Ridge National Laboratory, 1 Bethel Valley Road, Oak Ridge, TN 37831, USA*
(Dated: March 11, 2011)

Inelastic neutron scattering was used to measure phonon spectra on MgB_2 and $Mg_{0.75}Al_{0.25}B_2$ from 7 K to 750 K to investigate anharmonicity and adiabatic electron-phonon coupling. First principles calculations of phonons with a linear response method were performed at multiple unit cell volumes, and the Helmholtz free energy was minimized to obtain the lattice parameter and phonon dynamics at elevated temperature in the quasiharmonic approximation. Most of the temperature-dependence of the phonon DOS could be understood with the quasiharmonic approximation, although there was also significant thermal broadening of the phonon spectra. In comparison to $Mg_{0.75}Al_{0.25}B_2$, in the energy range of 60 to 80 meV the experimental phonon spectra from MgB_2 showed a non-monotonic change with temperature around 500 K. This may originate from a change with temperature of the adiabatic electron-phonon coupling.

I. INTRODUCTION

Superconductivity in magnesium diboride (MgB_2)[1] has attracted widespread attention. Phonon mediated electron pairing was early suspected as the mechanism of superconductivity, although the superconducting transition temperature $T_c \approx 39$ K would be the highest known for this mechanism. Soon it was established that the superconductivity of MgB_2 has a two band character and BCS-type electron pairing[2–9] with unusually strong, anisotropic electron-phonon coupling[7–13]. It was shown that electron states in the covalent σ band, originating with in-plane boron sp^2 hybridized orbitals, couple very strongly to the E_{2g} phonon mode with its in-plane B-B bond stretching[9,13,14].

Nevertheless, several aspects of superconductivity in MgB_2, including the importance of phonon anharmonicity, are not fully understood and remain controversial. First principles calculations of the E_{2g} phonon frequency at Γ, based on the harmonic approximation, significantly underestimate numerous Raman spectroscopy measurements[15–21]. Frozen-phonon calculations[4,6,7,9,12,13,22,23], are in excellent agreement at 0 K, and attribute this discrepancy to the onset of anharmonicity. Anharmonicity could play a significant role in explaining the high T_c and small isotope effect[3,24]. Later calculations, based on a more rigorous perturbation theory approach, showed that the effects of anharmonicity are much smaller, owing to a negative contribution of the three-phonon scattering term[20,23], in accord with more recent inelastic x-ray scattering and tunneling spectroscopy measurements[14,20,25,26]. Today the thermal shifts and broadenings of Raman peaks have not yet been related to the phonon dynamics, and await theoretical explanation[19–21,27–29].

Non-harmonic behavior is generally expected at high temperatures, and interesting thermodynamic effects can occur when temperature causes changes in the electron-phonon interaction (EPI) or phonon-phonon interaction (PPI). A phonon distorts a crystal, and the potential energy of this distortion can be considered all electronic in origin, but the kinetic energy of the phonon is in the motion of the nuclei. For a harmonic phonon, the EPI affects equally the energies of the electrons and the phonons. The "adiabatic" EPI requires simultaneous thermal excitations of both electrons and phonons. The strong EPI of MgB_2 may affect its thermodynamics at high temperatures because the adiabatic EPI may be expected to change with temperature, much as was found for superconducting transition metals[30–32]. To date, studies on phonon dynamics[9,14,15,17–21,25,26,33] and lattice expansion[18,34–38] of MgB_2 have been limited to temperatures 300 K or below.

The electronic structure near the Fermi energy is sensitive to the lattice constants a and c, and to the amplitude of boron atom displacements[22,39]. The anharmonicities of the E_{2g} phonon modes are affected by the positions of partially-filled boron σ bands relative to the Fermi level[9,22]. Substituting Al for Mg lowers the critical temperature for superconductivity, and it was previously shown that the phonon DOS of $Mg_{1-x}Al_xB_2$ is very sensitive to the concentration of Al[12,40]. This was attributed to Al donating its $3p$ electrons to the sp^2 "hole pockets" of MgB_2. The filling of the hole pockets by Al doping is expected to affect the electronic screening of B atom displacements, altering the interatomic forces between B atoms. Another effect of Al doping should be to alter the temperature-dependence of the EPI, since the thermal broadening of electron occupancies and the thermal lifetime broadening of electron levels will change with band filling. This should be reflected in differences in the temperature dependence of the phonon density of states.

Here we present results from experimental and computational work on MgB_2 at elevated temperatures. Neutron-weighted densities of states (NWDOS) were obtained from inelastic neutron scattering (INS) spectra measured on MgB_2 and $Mg_{0.75}Al_{0.25}B_2$ to identify the effects of doping. *Ab-initio* calculations were performed for MgB_2, $MgAlB_4$, and AlB_2, using the quasi-harmonic (QH) approximation. The lattice dynamics of MgB_2 can be mostly understood with the QH approximation, but non-harmonic behavior is found for phonons in the energy region of the E_{2g} phonon modes of MgB_2.

II. EXPERIMENTAL

The samples were synthesized by direct reaction of turnings of 99.98% pure Mg, 99.5% pure Al powders of 325 mesh, and 100 mesh powders of 98.78% isotopically-enriched ^{11}B. The elements were enclosed in tantalum cylinders with welded seals, and reacted for 1 h at 1073 K, and then for 2 h at 1223 K in quartz tubes under an argon atmosphere. The product was ground into a fine powder and annealed in the same way at 1223 K for 15 h. The sample was finally annealed under dynamic vacuum at 750 K for 8 hours to remove any unreacted Mg. Rietveld refinement of the XRD patterns showed the materials to have phase purities of 95%, with the main impurity phases being MgB_4 (3%) and MgO (2%).

Inelastic neutron scattering (INS) measurements were performed with the wide Angular-Range Chopper Spectrometer (ARCS) of the Spallation Neutron Source (SNS) at the Oak Ridge National Laboratory. For all results reported here, about 10 g of MgB_2 or $Mg_{0.75}Al_{0.25}B_2$ powders were accommodated in an annular aluminum can with an outer diameter of 2.9 and an inner diameter of 2.7 cm, resulting in the scattering of about 10% of the incident neutron beam.

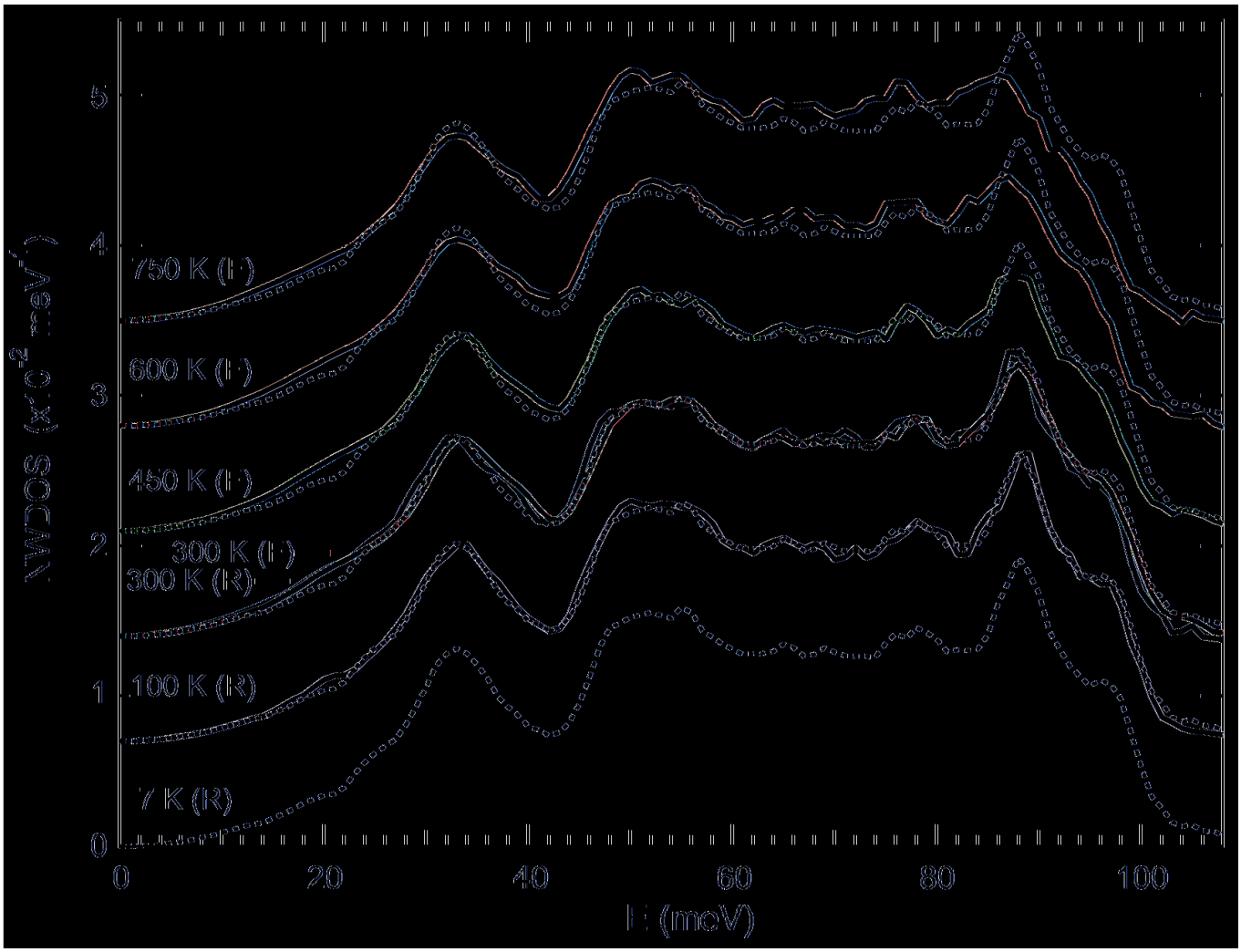

FIG. 1. Neutron-weighted phonon DOS of MgB_2 from INS data measured at temperatures as labeled, with sample in furnace (F) or refrigerator (R). Dotted lines, next to the higher temperature curves, correspond to the 7 K result, shifted by a constant.

The sample was mounted in either a closed-cycle helium refrigerator or a low-background resistive furnace with thin aluminum shielding for thermal radiation, and neutron-absorbing boron nitride to suppress extraneous scattering. The nominal incident energy for all measurements was 165 meV. The energy resolution (FWHM) was 3.0 meV at 100 meV neutron energy loss, increasing to 7.2 meV at the elastic line. Neutron diffraction patterns, obtained by integrating the elastic part of the data (from –5 to 5 meV), gave lattice parameters in agreement with the literature and our XRD measurements, and showed no evidence of any phase transitions as a function of temperature.

The raw INS data were re-binned into intensity I as a function of momentum transfer Q and energy transfer E. Differences in efficiency between detectors were corrected with measurements on a vanadium rod. Neutron-weighted phonon densities of states (NWDOS) curves were calculated from the $I\,(Q, E)$ in the incoherent scattering approximation. The measured background was subtracted and an iterative procedure was used to remove contributions from multiple scattering and higher order multi-phonon processes[41,42]. The analysis includes corrections for Bose-Einstein and Debye-Waller factors. The neutron weights for phonon scattering are the ratios of neutron cross section over mass σ/M, which are 0.153 and 0.534 barns/amu for Mg and B, respectively, so the motions of B atoms are over-emphasized by a 7:1 ratio for MgB_2. Results are shown in Figs. 1 and 2.

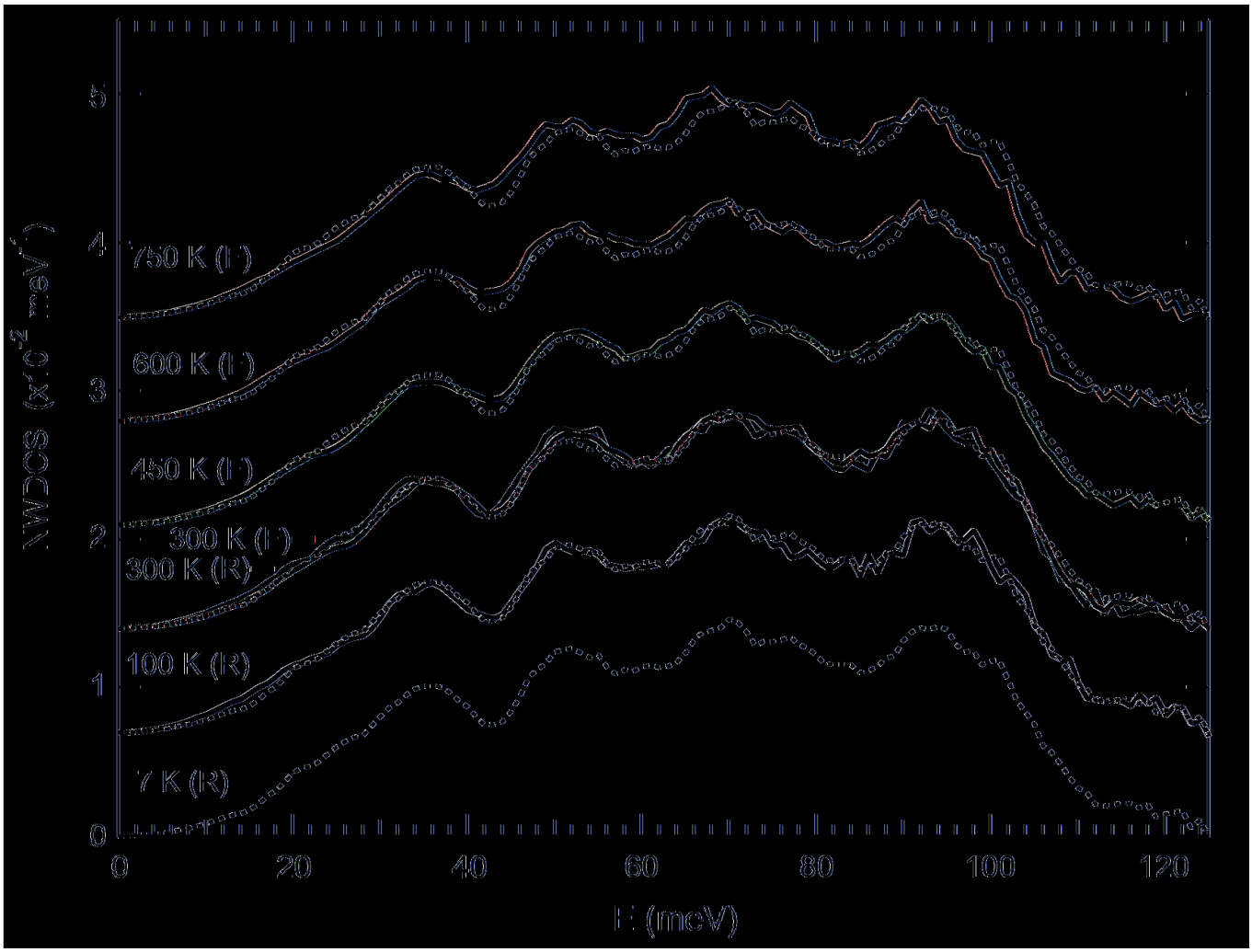

FIG. 2. Neutron-weighted phonon DOS of $Mg_{0.75}Al_{0.25}B_2$ from INS data measured at temperatures as labeled, with sample in furnace (F) or refrigerator (R). Dotted lines, next to the higher temperature curves, correspond to the 7 K result, shifted by a constant.

III. COMPUTATIONAL

Electronic structure calculations[43] were performed with density functional theory (DFT) in the generalized gradient approximation[44]. For computationally feasible energy cutoffs, all calculations used ultrasoft[45] pseudopotentials for B, and norm conserving pseudopotentials[46] for Mg and Al. An energy cutoff of 64 Ry was used in the plane wave expansion and charge density cutoff of 256 Ry with Monkhorst-Pack[47] 32×32×32 k-point grids for MgB_2, AlB_2, and 32×32×16 for $MgAlB_4$. A Methfessel-Paxton[48] smearing of 0.015 Ry for Brillouin zone integration was used to ensure adequate convergence of energy and phonon frequencies for free energy minimization in the quasiharmonic model. The phonon calculations were performed on relaxed structures. The lattice parameters obtained for MgB_2, $MgAlB_4$, and AlB_2 were $a = 3.063$ Å and $c = 3.482$ Å, $a = 3.030$ Å and $c = 6.694$ Å, $a = 3.001$ Å and $c = 3.273$ Å, respectively, in good agreement with experiments[34,35,49,50]. Phonon frequencies and eigenmodes were calculated using the linear response technique[51]. The dynamical matrices for calculations on fine meshes were obtained from a Fourier interpolation of the dynamical matrices computed on 6×6×6 phonon meshes. Phonon densities of states then were computed on 28×28×28 meshes using the tetrahedron scheme.

To calculate the effects of thermal expansion on phonons, we used the quasiharmonic (QH) approximation. The QH approximation assumes phonons to be harmonic, and effects of non-harmonicity enter through the volume dependence. Quasiharmonicity may be the major contributor to many thermodynamic properties at elevated temperatures, if the theoretical model is of sufficient quality[52]. We performed a series of calculations at increasing volumes. At each volume, the lattice parameters a and c and the atomic positions in the unit cell were independently optimized to

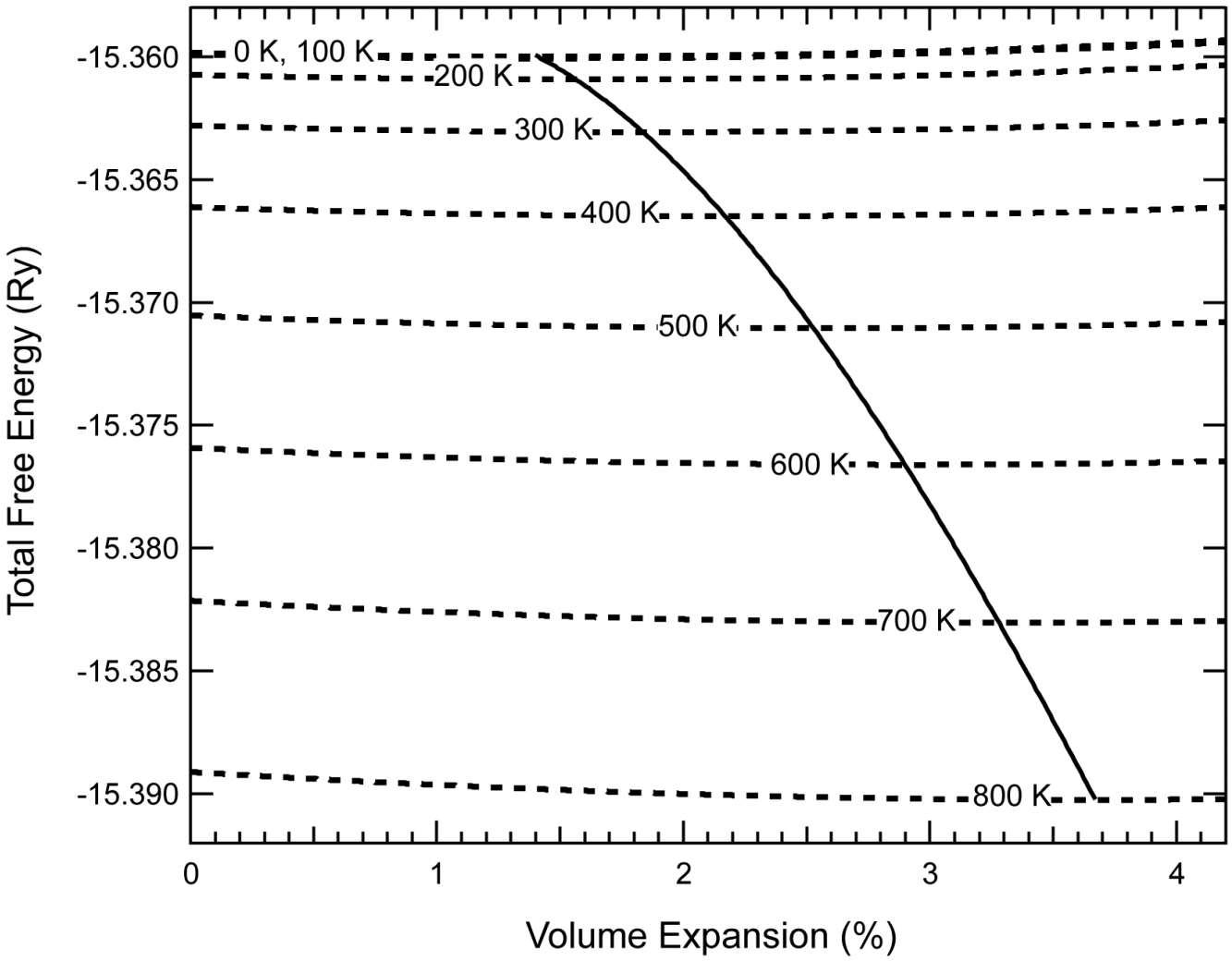

FIG. 3. Computed Helmholtz free energy (total, electronic plus phonon) as a function of volume expansion. Line crossings show energy minima at different temperatures.

minimize the electronic energy, $U_{\rm el}(V)$, which was then fitted using the Birch-Murnaghan equation of state. Phonon free energies were computed from the calculated phonon DOS using the harmonic approximation

$$F_{\rm ph}(T,V) = \int \left[\frac{\hbar\omega}{2} + k_{\rm B}T \ln\left(1 - {\rm e}^{-\frac{\hbar\omega}{k_{\rm B}T}}\right)\right] g_V(\omega)\,{\rm d}\omega \ , \qquad (1)$$

where $g_V(\omega)$ is a phonon DOS from a DFT linear response calculation at a specific volume. At each temperature, the free energy of Eq. 1 was fitted to a polynomial in V, and the minimum value of the Helmholtz free energy, $F_{\rm tot}(T,V) = U_{\rm el}(V) + F_{\rm ph}(T,V)$, was used to obtain the optimal volumes and lattice parameters at fixed temperatures as shown in Fig. 3. Note the substantial effect from the zero-point energy.

IV. RESULTS

Figure 4 presents the thermal expansion, $\Delta a/a_0$ and $\Delta c/c_0$ of MgB_2 from calculations in the QH approximation, and from experiment. Our experimental data, obtained from 325−898 K, match well with prior results from lower temperatures[34,35]. Our lattice parameters at room temperature were $a_{\rm RT} = 3.0856$ Å and $c_{\rm RT} = 3.5239$ Å, in a good agreement with $a_{297{\rm K}} = 3.08489$ Å from[34] and $c_{\rm RT} = 3.52196$ Å from[35]. The calculated thermal expansions are in good agreement with experiment to 900 K and, like in earlier reports[18,34–38], are about twice as large along c than along a.

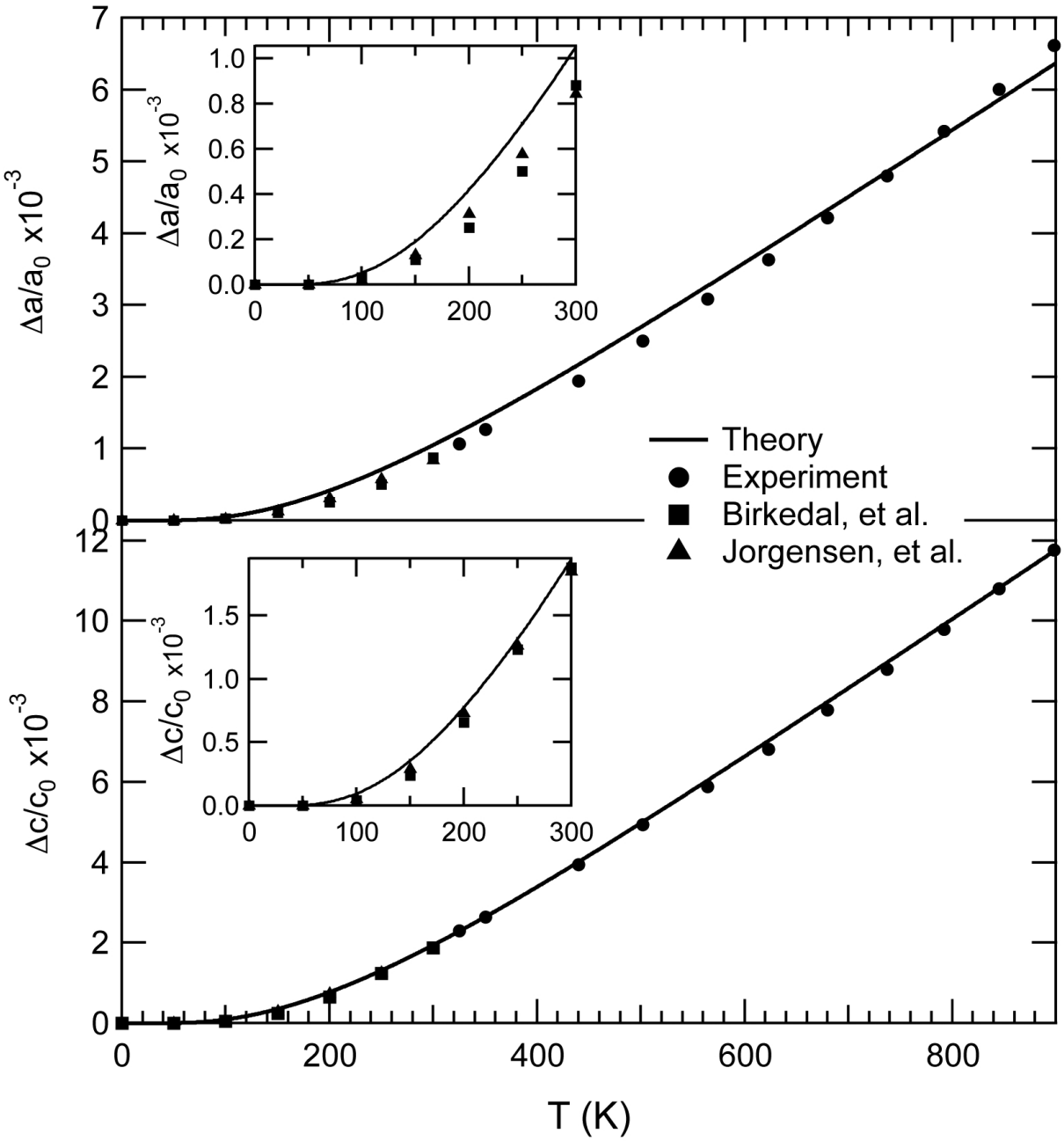

FIG. 4. Linear thermal expansion $\Delta L/L_{0K}$ of MgB_2 in the QH approximation for the a-axis (upper) and c-axis (lower), in comparison with the present experiment and earlier reports[34,35]. Insets enlarge the low-temperature region.

The neutron-weighted phonon densities of states (NWDOS) of MgB_2 and $Mg_{0.75}Al_{0.25}B_2$ (Figs. 1 and 2) from measurements with samples in the closed cycle refrigerator (CCR) at 7 K, 100 K and 300 K are very similar, and show the small variability of the experimental results. There were some differences in background between the spectra from measurements in the refrigerator at 300 K and in the furnace at 300 K, but the changes in spectra from the furnace measurements can be identified reliably. For measurements at 300 K and below, the NWDOS are in good agreement with published results[9,33,40]. At 600 and 750 K the NWDOS curves broaden noticeably in the energy region of 60−95 meV, and the high energy peak softens considerably.

A set of NWDOS curves were obtained as follows from the first principles calculations. The calculated phonon partial DOS curves of the individual elements were multiplied by appropriate neutron weighting factors and summed. Next, they were convolved with an energy-dependent experimental resolution function characteristic of the ARCS

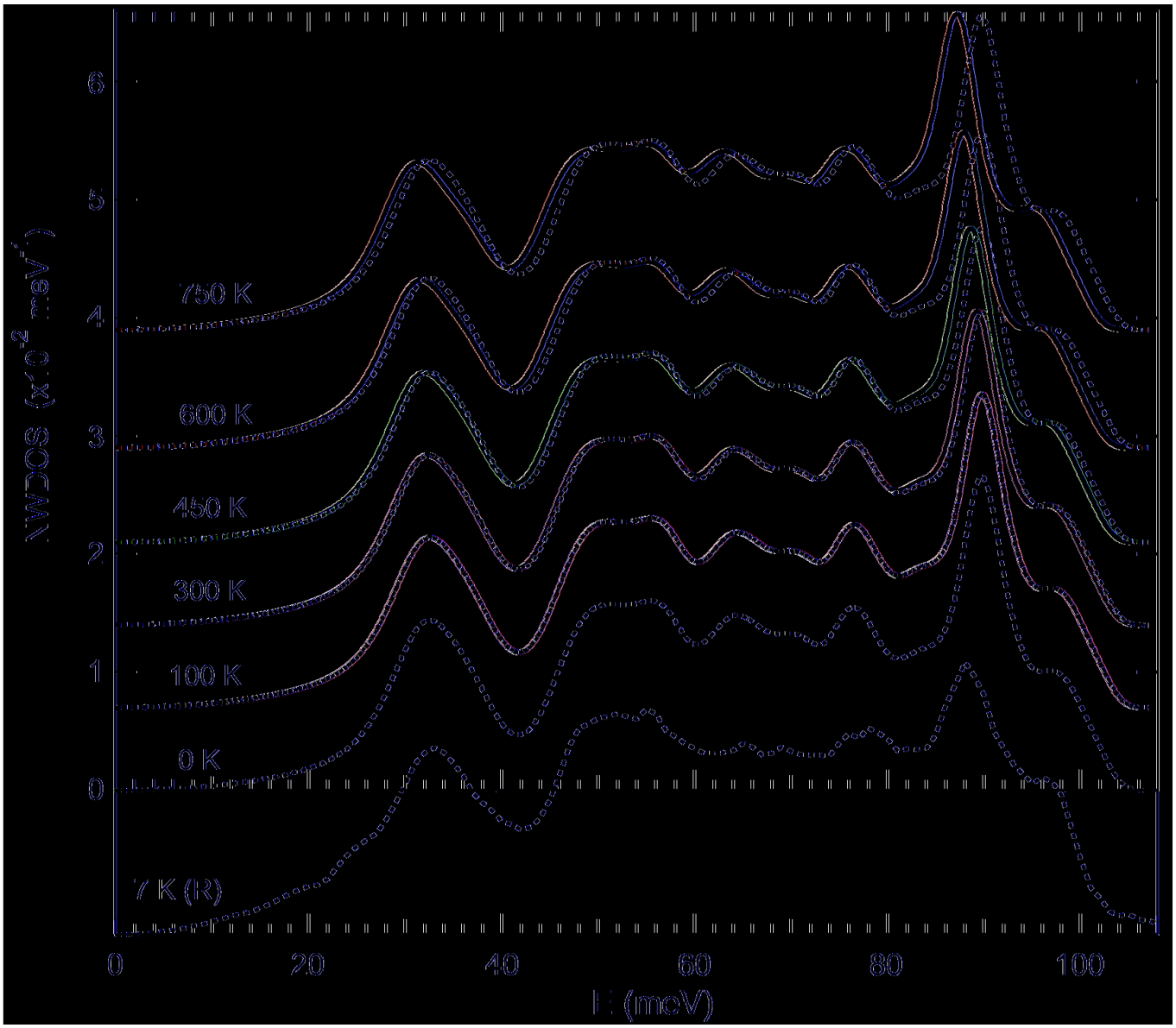

FIG. 5. Temperature dependence of computed NWDOS of MgB_2 in the QH approximation. Curve appended at bottom is an experimental curve from Fig. 1. Dotted lines, next to the higher temperature curves, correspond to the 7 K result, shifted by a constant.

spectrometer. The calculated NWDOS curves are shown in Fig. 5. The thermal trends are generally consistent with our experimental results from Fig. 1, although thermal broadening does not occur in the QH approximation, and broadening from the zero-point motions is also missing. The thermal shifts for the QH NWDOS calculated for $MgAlB_4$ were similar, although a bit smaller.

The experimental NWDOS curves of MgB_2 and $Mg_{0.75}Al_{0.25}B_2$ (Figs. 1 and 2) were analyzed with a simple model that assumes all phonons shift in energy quasiharmonically with one Grüneisen parameter, γ, and broaden with temperature as damped harmonic oscillators, $D(\mathcal{Q}, E', E)$, with a single quality factor, $\mathcal{Q}$[41,42]. To get each high temperature NWDOS, g_T, the experimental NWDOS curve obtained at 7 K was recalled in energy through γ, and convolved with a Lorentzian with half-width-at-half-maximum $\Gamma = \omega/2\mathcal{Q}$ at each energy: $g_T(E) = D(\mathcal{Q}, E', E) * g_{7K}((1+\gamma)E')$ and renormalized. The parameters γ and $\mathcal{Q}$ were optimized for best fits to the NWDOS curves at higher temperatures. The results were generally successful, as shown by the results of Fig. 6 for MgB_2, which includes the modeled and actual differences between the NWDOS curves at 7 K and 750 K. Also shown is the difference between the *ab-initio* quasiharmonic results for the same temperatures. The two quasiharmonic approaches are in reasonable agreement with each other, although the sharper features in the *ab-initio* NWDOS curves give large

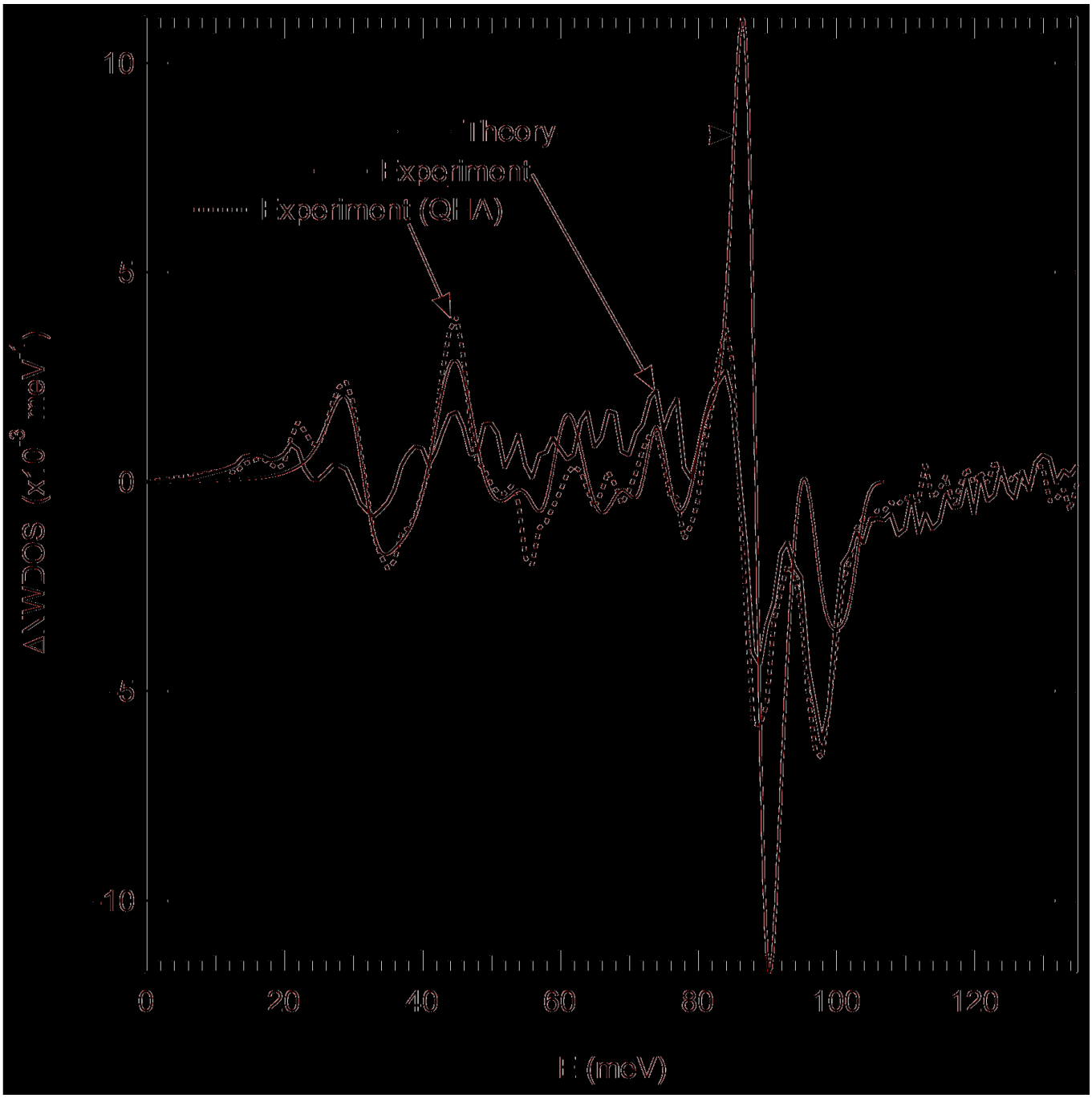

FIG. 6. Differences of NWDOS curves of MgB_2 at 7 K and 750 K. Experiment is from actual NWDOS curves, Experiment (QHA) is from the difference using a 750 K curve from two-parameter modification of the 7 K experimental data (see text), and Theory is the difference between the curves computed by *ab-initio* QH theory. The experimental curves were corrected for the differences between the spectra acquired from samples in the furnace and refrigerator at 300 K.

difference peaks from 80 to 95 meV. The experimental difference of NWDOS curves of MgB_2 shows some differences, including a broad difference over the energy range from 50 to 80 meV. Figure 7 shows the difference between the differential experimental and theoretical NWDOS curves $\Delta\Delta$NWDOS(T)=ΔNWDOS$_{\rm Exp}$(T)-ΔNWDOS$_{\rm Theor}$(T), at different temperatures. Overall, there is a good correspondence, and no significant shifts throughout the energy range. The plot displays some changes of shape with temperature in the 50 to 80 meV region, and noticeable shifting around 84 meV, caused by the asymmetrical broadening of the corresponding experimental peak (Figure 1).

Computed dispersions of phonons and Grüneisen parameters for MgB_2 are presented in Fig. 8. The phonon

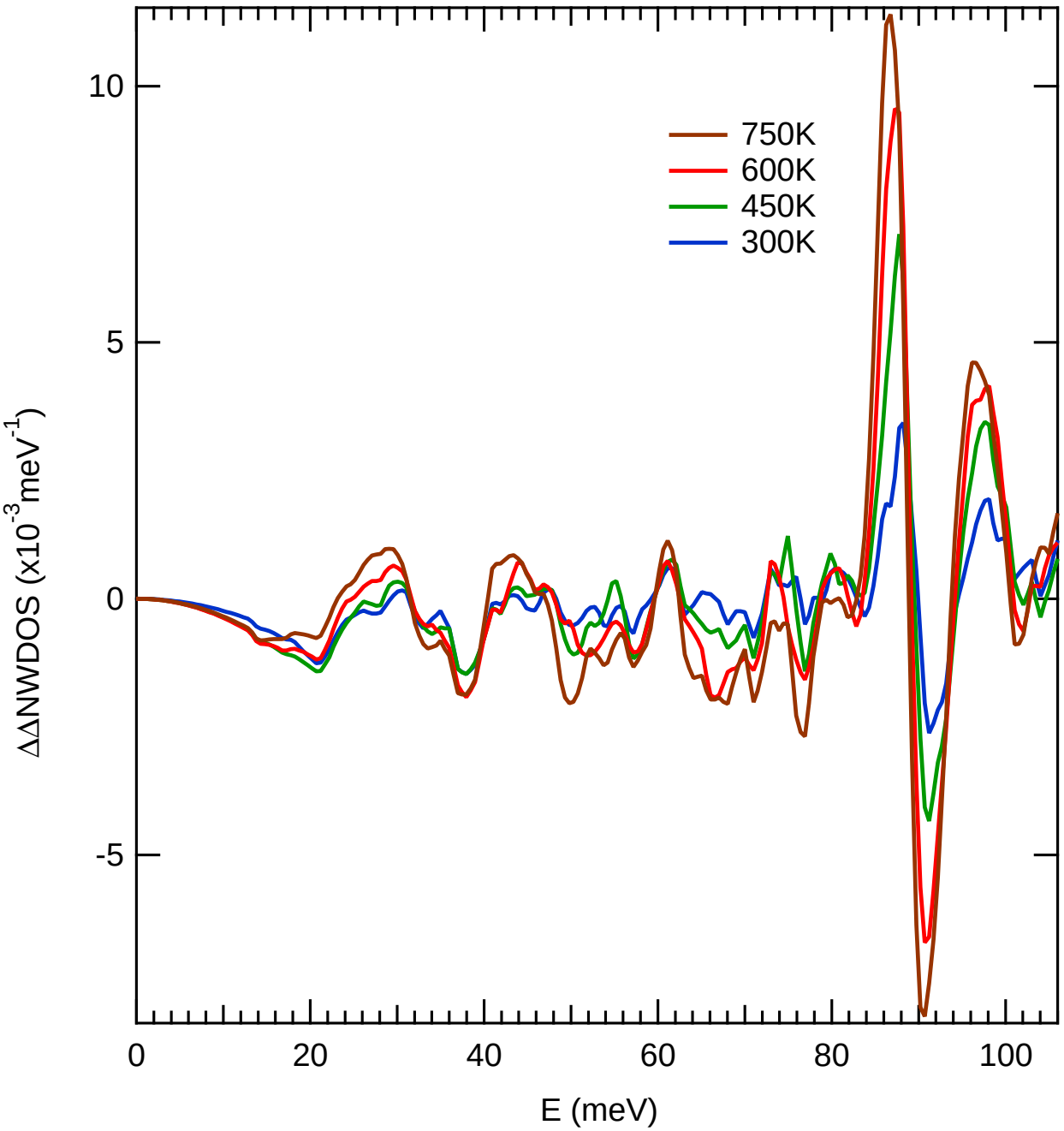

FIG. 7. Difference between ΔNWDOS (Experiment, Fig. 6) and ΔNWDOS (Theory, Fig. 6) at temperatures as labeled.

dispersions are in good agreement with previous work[15,23]. The Grüneisen parameters were obtained by fitting phonon frequencies obtained at 0 K for a series of volume expansions up to 0.1% from equilibrium: $(\omega/\omega_0 - 1) = -\gamma(V/V_0 - 1) + \chi(V/V_0 - 1)^2 + \ldots$. The calculated Grüneisen parameters (Fig. 8) are all positive, but highly anisotropic. Our calculations of dispersions along the $\Gamma - A$ direction for three compounds of different Al concentration are presented in Fig. 9. The phonon frequencies, especially of E_{2g} modes, are very sensitive to the Al concentration in Mg-rich material, as was pointed out earlier[40]. In comparison to AlB_2 and $MgAlB_4$, the E_{2g} modes of MgB_2 along the $\Gamma - A$ direction have low frequencies and large Grüneisen parameters. Nevertheless, other modes contribute to the NWDOS in the energy range from 60 to 80 meV, and the net effect of this large quasiharmonic phonon softening in Fig. 5 is modest.

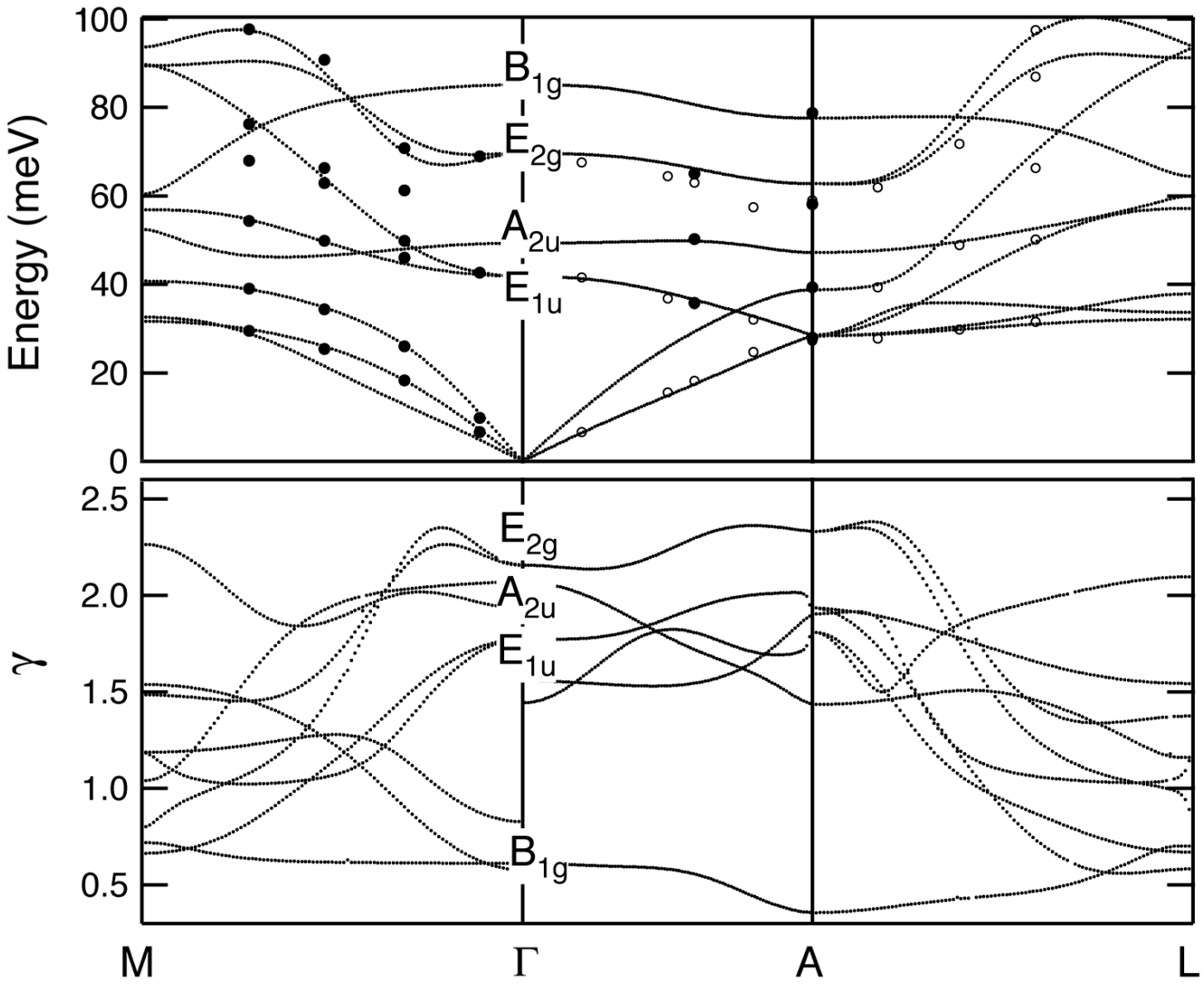

FIG. 8. Upper panel: MgB_2 calculated phonon dispersions compared with experimental results from Ref.[20] (filled circles) and Ref.[14] (open circles). Bottom panel: calculated dispersions of Grüneisen parameter γ.

V. DISCUSSION

The features of the NWDOS curves for $Mg_{0.75}Al_{0.25}B_2$ (Fig. 2) shift systematically to lower energies with temperature, consistent with a quasiharmonic model. The difference spectra of Fig. 10 for $Mg_{0.75}Al_{0.25}B_2$ show the characteristics of peak broadenings and shifts to lower energies, where there is increased intensity on the low-energy side of a peak and a sharper loss of intensity on the high-energy side. The prominent changes in the difference spectra of MgB_2 from 80 to 100 meV increase monotonically with temperature.

The high sensitivity of the E_{2g} modes to relatively small amounts of Al concentration in Mg-rich alloys is understood as an effect of electronic structure on interatomic forces. We have some evidence that temperature plays a similar role. Our theoretical calculations on MgB_2 based on the quasiharmonic model (Fig. 5) show that all features in the phonon DOS soften monotonically with temperature. The differences of experimental spectra (Fig. 6) show less consistency with the computed quasiharmonic results or with the linearly scaled and broadened NWDOS. Some differences, such as the narrow peaks from 80 to 100 meV, originate primarily with the sharpness of the peaks in the calculated DOS. In the energy range from 60 to 80 meV, however, the extra intensity in the experimental difference curve requires some modes moving down into this energy range from above, and perhaps up from below. Unlike the calculated results, the temperature dependence of the experimental difference spectra from 60 to 80 meV is different for MgB_2 and $Mg_{0.75}Al_{0.25}B_2$ (Fig. 10). Compared to the low-temperature NWDOS, the NWDOS of MgB_2 shows

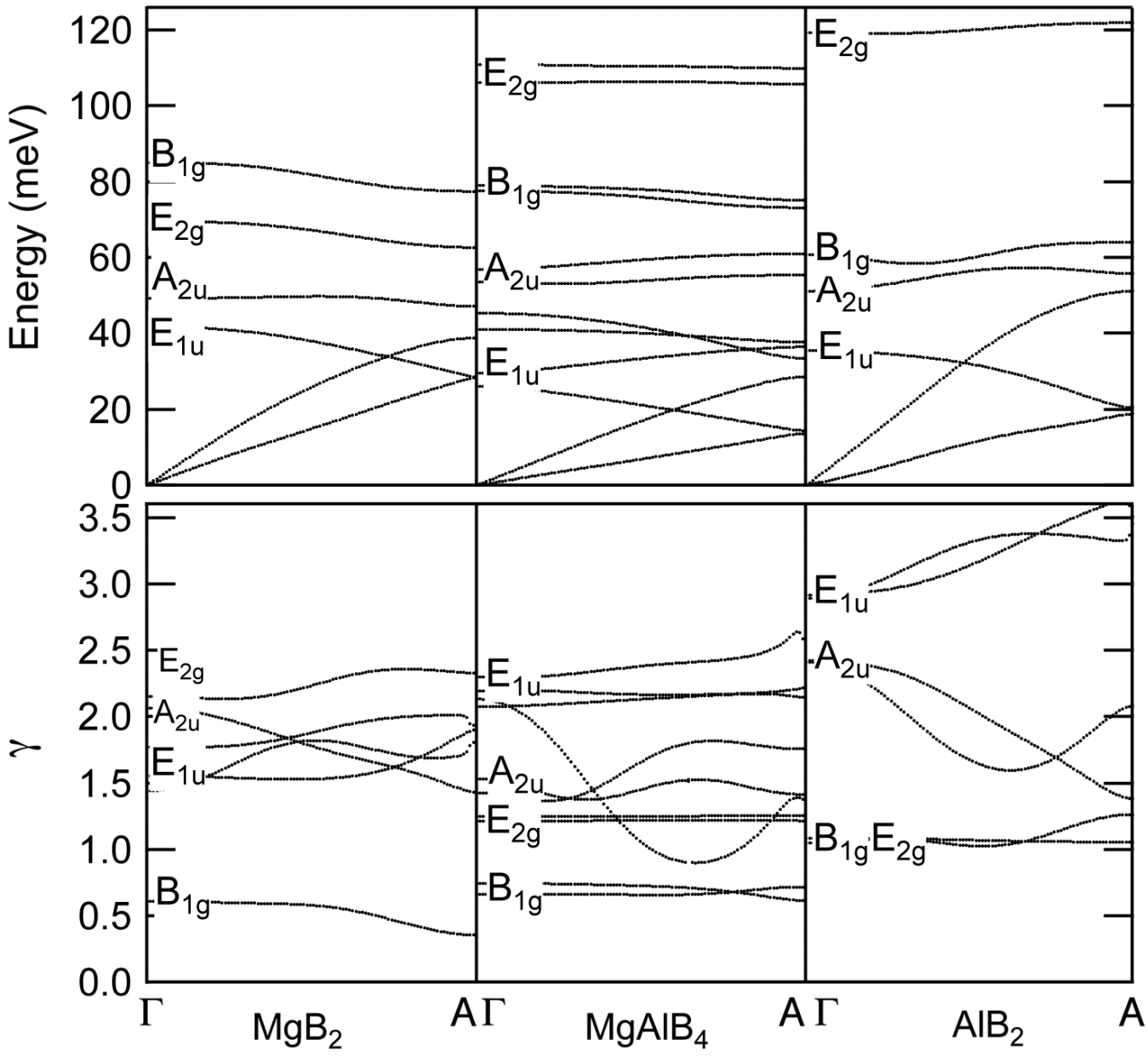

FIG. 9. Comparison of calculated dispersions (upper panel) and Grüneisen parameters γ along $\Gamma - A$ direction.

relatively little change at 450 K, but differs strongly at 600 and 750 K. The difference spectra of $Mg_{0.75}Al_{0.25}B_2$ are more monotonic with temperature. These effects are small, but are larger than the variations of the measured spectra. The energy range of 60 to 80 meV includes the E_{2g} boron modes along $\Gamma - A$, which have strong electron-phonon coupling. It is possible that some phonon softening from the adiabatic electron-phonon coupling is lost as the electron DOS near the Fermi level is broadened with temperature. The temperature range for this change seems to be between 500 and 600 K, above which a monotonic change is seen again in the difference spectra of MgB_2. Concerning the large broadening of the peak at 95 meV (Fig. 1), there is an evidence[14] that the third order anharmonicity of the E_{2g} mode is sensitive to temperature, and could perhaps be responsible for the broadening.

To understand the possible role of anharmonicity from phonon-phonon interactions, we calculated the behavior of a single E_{2g} mode, which does not contain third order anharmonicity[9,15,22]. The calculations were performed with the frozen phonon approximation at the Γ point[6,7,9,13,15,22]. This approximation is reported to heavily overestimate the absolute value of frequency shift[23], but we are interested in its relative change with temperature. At each lattice expansion obtained from the QH model, we generated the potential surface along the effective coordinate of the mode,

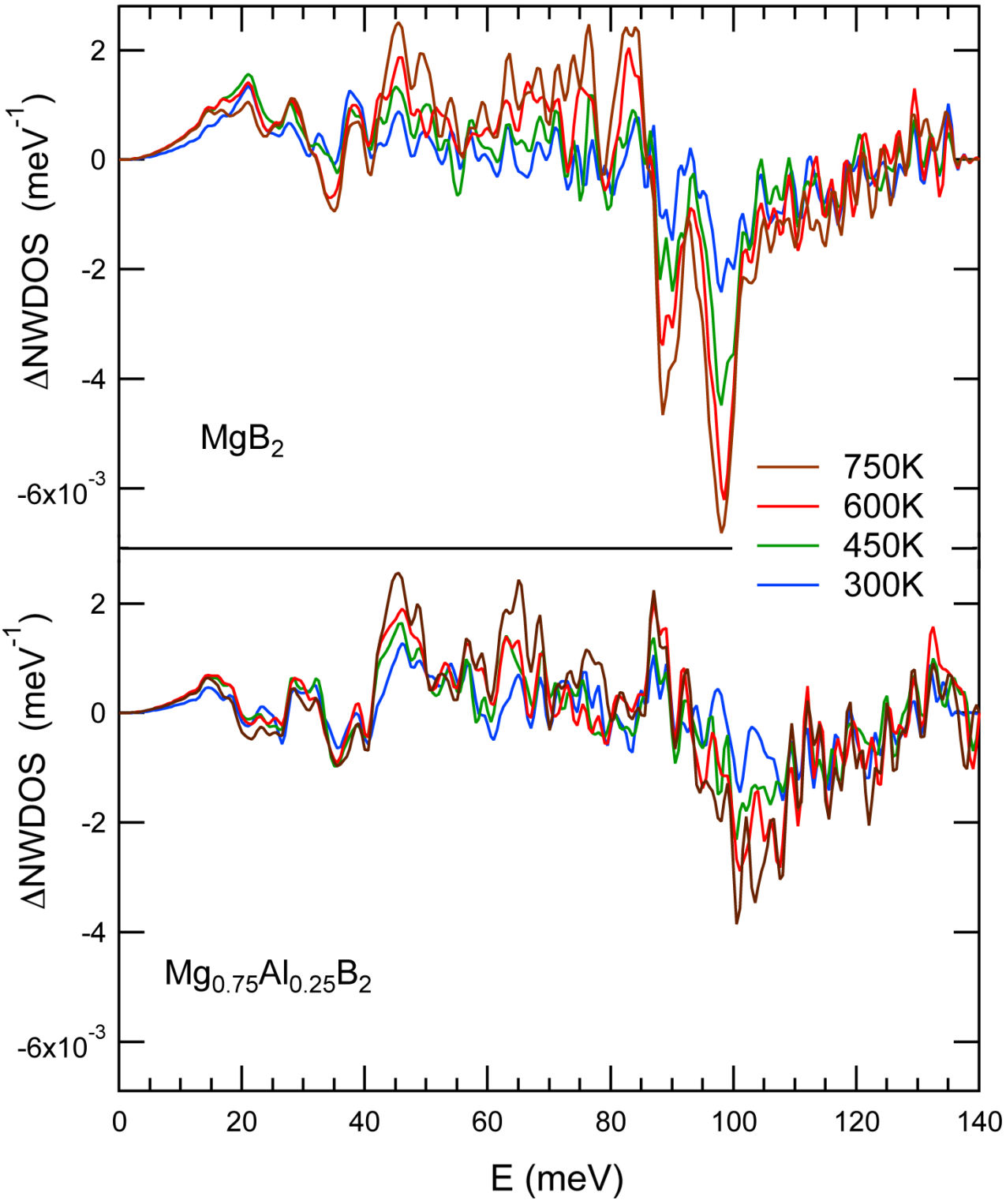

FIG. 10. Difference spectra of NWDOS of MgB_2 and $Mg_{0.75}Al_{0.25}B_2$ in the 300-750 K temperature range. The experimental curves were corrected for the differences between the spectra acquired from samples in the furnace and refrigerator at 300 K.

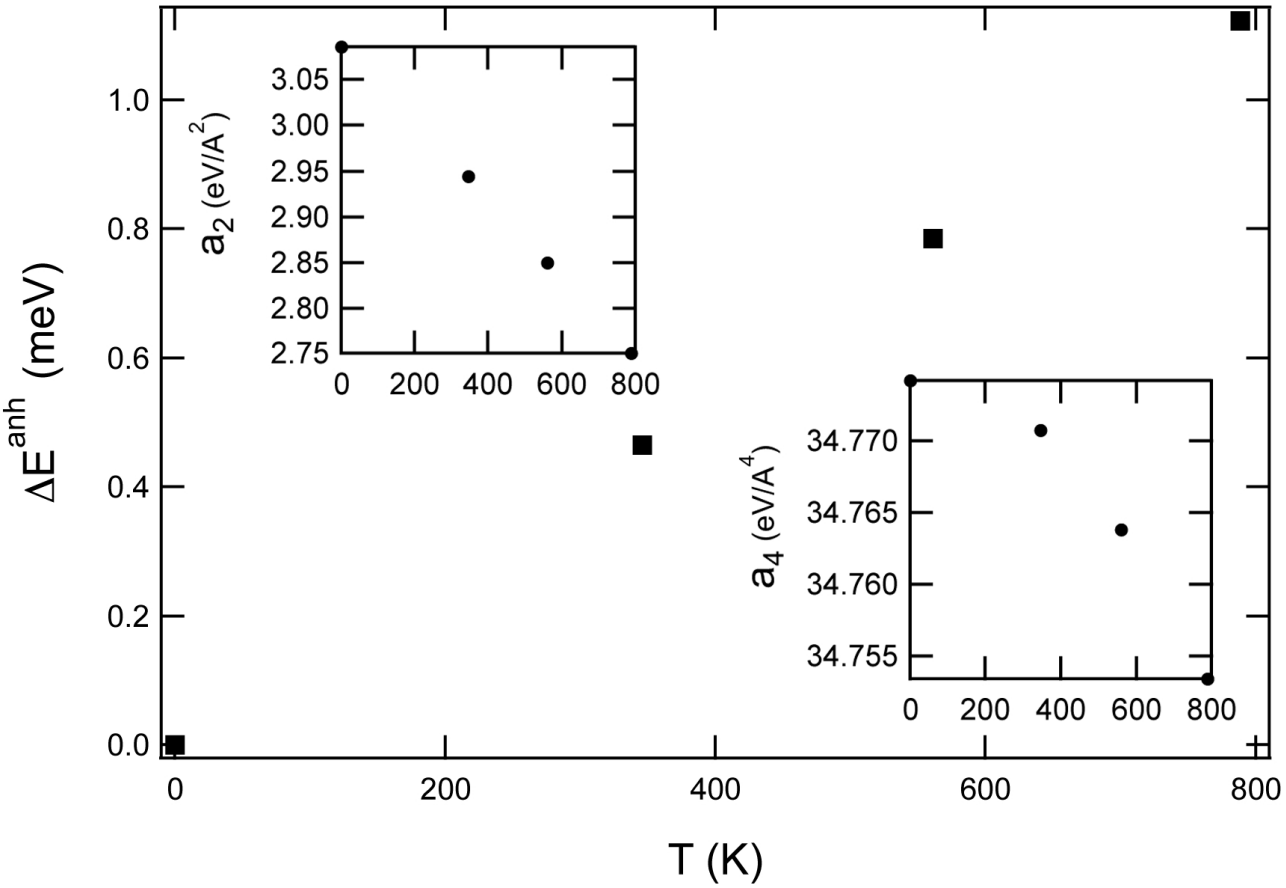

FIG. 11. Shift of $E^{\rm anh} = E^{\rm tot} - E^{\rm QH}$ for E_{2g} mode relative to 0 K, $\Delta E^{\rm anh} = E^{\rm anh}(T) - E^{\rm anh}(0K)$. Insets display the variation of the fitting parameters for the E_{2g} potential surface.

u, and fitted it with the potential to a polynomial of form $a_2u^2 + a_4u^4$. The phonon energies $E_{\rm tot}$ were computed by solving the secular problem. We obtain an anharmonic phonon energy shift of 9.24 meV at 0 K, in good agreement with 9.46 meV from previous work[23]. A measure of anharmonicity is the ratio of the quartic to squared quadratic coefficient, $a_4/a_2^2 = 3.6\,{\rm eV}^{-1}$. This is on the lower bound of $4{-}8\,{\rm eV}^{-1}$ from Refs.[9,15]. Figure 11 shows that the anharmonic energy shift increases slowly with temperature. At 0.46 meV at 300 K, it is smaller than a previous report of 1.22 meV[23], using experimental lattice parameters at 0 and 300 K. Using fourth-order phonon-phonon perturbation theory, the same authors obtained 0.38 meV. At 750 K, our frozen phonon model gives an anharmonic phonon energy shift of 0.66 meV. This could account for some of the non-quasiharmonic effects seen in the NWDOS of MgB_2 at high temperatures, but these anharmonic effects are small and without the third-order anharmonicity they may be overestimated. Furthermore, they are monotonic with temperature, so it seems most likely that the effects of temperature on phonons in the energy range of 60 to 80 meV originate with the temperature dependence of the EPI.

VI. CONCLUSION

Phonon spectra were measured on MgB_2 and $Mg_{0.75}Al_{0.25}B_2$ at temperatures from 7 K to 750 K, showing a broadening and general softening of the phonon DOS. The average behavior can be explained by the quasiharmonic model, where a free energy is obtained for a solid that expands because its lower phonon entropy counteracts the energy cost of expansion. *Ab-initio* free energy calculations were performed to predict the phonon softening in the quasiharmonic model, and were generally successful for MgB_2. Significant thermal broadenings of the phonons in MgB_2 were observed, however, inconsistent with the quasiharmonic approximation. A frozen phonon calculation performed at the Γ point gave small effects from phonon anharmonicity that increase the phonon energy with temperature. These quasiharmonic and anharmonic effects are monotonic with temperature, and the neutron-weighted phonon DOS of

MgB_2 showed a non-monotonic behavior between 425 K and 600 K that may be related to a change with temperature in the electron-phonon interaction. The effect is small, however, and difficult to discern from the measured spectra. Neither the phonon-phonon anharmonicity nor the electron-phonon interaction make substantial contributions to the vibrational entropy of MgB_2.

ACKNOWLEDGMENTS

This work was supported by the Department of Energy through the Basic Energy Sciences Grant DE-FG02-03ER46055. The portions of this work conducted at Oak Ridge National Laboratory were supported by the Scientific User Facilities Division and by the Division of Materials Sciences and Engineering, Office of Basic Energy Sciences, DOE. This work benefitted from DANSE software developed under NSF Grant No. DMR-0520547.

[1] J. Nagamatsu, N. Nakagawa, T. Muranaka, Y. Zenitani, and J. Akimitsu, Nature **410**, 63 (2001).
[2] C. Buzea and T. Yamashita, Superconductor Science and Technology **14**, R115 (2001).
[3] S. L. Bud'ko, G. Lapertot, C. Petrovic, C. E. Cunningham, N. Anderson, and P. C. Canfield, Phys. Rev. Lett. **86**, 1877 (2001).
[4] H. Choi, D. Roundy, H. Sun, M. Cohen, and S. Louie, Nature **418**, 758 (2002).
[5] S. Tsuda, T. Yokoya, Y. Takano, H. Kito, A. Matsushita, F. Yin, J. Itoh, H. Harima, and S. Shin, Phys. Rev. Lett. **91**, 127001 (2003).
[6] A. Y. Liu, I. I. Mazin, and J. Kortus, Phys. Rev. Lett. **87**, 087005 (2001).
[7] J. Kortus, I. I. Mazin, K. D. Belashchenko, V. P. Antropov, and L. L. Boyer, Phys. Rev. Lett. **86**, 4656 (2001).
[8] Y. Kong, O. V. Dolgov, O. Jepsen, and O. K. Andersen, Phys. Rev. B **64**, 020501 (2001).
[9] T. Yildirim, O. Gülseren, J. W. Lynn, C. M. Brown, T. J. Udovic, Q. Huang, N. Rogado, K. A. Regan, M. A. Hayward, J. S. Slusky, T. He, M. K. Haas, P. Khalifah, K. Inumaru, and R. J. Cava, Phys. Rev. Lett. **87**, 037001 (2001).
[10] J. M. An and W. E. Pickett, Phys. Rev. Lett. **86**, 4366 (2001).
[11] P. P. Singh, Phys. Rev. Lett. **87**, 087004 (2001).
[12] K. P. Bohnen, R. Heid, and B. Renker, Phys. Rev. Lett. **86**, 5771 (2001).
[13] H. J. Choi, D. Roundy, H. Sun, M. L. Cohen, and S. G. Louie, Phys. Rev. B **66**, 020513 (2002).
[14] A. Shukla, M. Calandra, M. d'Astuto, M. Lazzeri, F. Mauri, C. Bellin, M. Krisch, J. Karpinski, S. M. Kazakov, J. Jun, D. Daghero, and K. Parlinski, Phys. Rev. Lett. **90**, 095506 (2003).
[15] K. Kunc, I. Loa, K. Syassen, R. K. Kremer, and K. Ahn, J. Phys.: Condensed Matter **13**, 9945 (2001).
[16] J. Hlinka, I. Gregora, J. Pokorný, A. Plecenik, P. Kus, L. Satrapinsky, and S. Benacka, Phys. Rev. B **64**, 140503 (2001).
[17] X. K. Chen, M. J. Konstantinović, J. C. Irwin, D. D. Lawrie, and J. P. Franck, Phys. Rev. Lett. **87**, 157002 (2001).
[18] L. Shi, H. Zhang, L. Chen, and Y. Feng, J. Phys.: Condensed Matter **16**, 6541 (2004).
[19] D. Di Castro, E. Cappelluti, M. Lavagnini, A. Sacchetti, A. Palenzona, M. Putti, and P. Postorino, Phys. Rev. B **74**, 100505 (2006).
[20] M. d'Astuto, M. Calandra, S. Reich, A. Shukla, M. Lazzeri, F. Mauri, J. Karpinski, N. D. Zhigadlo, A. Bossak, and M. Krisch, Phys. Rev. B **75**, 174508 (2007).
[21] A. Mialitsin, B. S. Dennis, N. D. Zhigadlo, J. Karpinski, and G. Blumberg, Phys. Rev. B **75**, 020509 (2007).
[22] L. Boeri, G. B. Bachelet, E. Cappelluti, and L. Pietronero, Phys. Rev. B **65**, 214501 (2002).
[23] M. Lazzeri, M. Calandra, and F. Mauri, Phys. Rev. B **68**, 220509 (2003).
[24] D. Hinks, H. Claus, and J. Jorgensen, Nature **411**, 457 (2001).
[25] A. Q. R. Baron, H. Uchiyama, Y. Tanaka, S. Tsutsui, D. Ishikawa, S. Lee, R. Heid, K.-P. Bohnen, S. Tajima, and T. Ishikawa, Phys. Rev. Lett. **92**, 197004 (2004).
[26] V. Y. Tarenkov, A. I. D'yachenko, S. L. Sidorov, V. A. Boichenko, D. I. Boichenko, S. Chromik, V. Strbik, S. Gazi, M. Spankova, and S. Benacka, Physics of the Solid State **51**, 1778 (2009).
[27] M. Calandra and F. Mauri, Phys. Rev. B **71**, 064501 (2005).
[28] E. Cappelluti, Phys. Rev. B **73**, 140505 (2006).
[29] A. M. Saitta, M. Lazzeri, M. Calandra, and F. Mauri, Phys. Rev. Lett. **100**, 226401 (2008).
[30] O. Delaire, M. S. Lucas, J. A. Muñoz, M. Kresch, and B. Fultz, Phys. Rev. Lett. **101**, 105504 (2008).
[31] O. Delaire, M. G. Kresch, J. A. Muñoz, M. S. Lucas, J. Y. Y. Lin, and B. Fultz, Phys. Rev. B **77**, 214112 (2008).
[32] B. Fultz, Prog. Mater. Sci. **55**, 247 (2010).
[33] R. Osborn, E. A. Goremychkin, A. I. Kolesnikov, and D. G. Hinks, Phys. Rev. Lett. **87**, 017005 (2001).
[34] J. D. Jorgensen, D. G. Hinks, and S. Short, Phys. Rev. B **63**, 224522 (2001).
[35] H. Birkedal, W. Van Beek, H. Emerich, and P. Pattison, J. Mater. Sci. Lett. **22**, 1069 (2003).
[36] R. Lortz, C. Meingast, D. Ernst, B. Renker, D. Lawrie, and J. Franck, J. Low Temp. Phys. **131**, 1101 (2003).
[37] Y. Xue, S. Asada, A. Hosomichi, S. Naher, J. Xue, H. Kaneko, H. Suzuki, T. Muranaka, and J. Akimitsu, J. Low Temp. Phys. **138**, 1105 (2005).

[38] J. J. Neumeier, T. Tomita, M. Debessai, J. S. Schilling, P. W. Barnes, D. G. Hinks, and J. D. Jorgensen, Phys. Rev. B **72**, 220505 (2005).
[39] X. Wan, J. Dong, H. Weng, and D. Y. Xing, Phys. Rev. B **65**, 012502 (2001).
[40] B. Renker, K. B. Bohnen, R. Heid, D. Ernst, H. Schober, M. Koza, P. Adelmann, P. Schweiss, and T. Wolf, Phys. Rev. Lett. **88**, 067001 (2002).
[41] M. Kresch, O. Delaire, R. Stevens, J. Y. Y. Lin, and B. Fultz, Phys. Rev. B **75**, 104301 (2007).
[42] M. Kresch, M. Lucas, O. Delaire, J. Y. Y. Lin, and B. Fultz, Phys. Rev. B **77**, 024301 (2008).
[43] P. Giannozzi, S. Baroni, N. Bonini, M. Calandra, R. Car, C. Cavazzoni, D. Ceresoli, G. L. Chiarotti, M. Cococcioni, I. Dabo, A. D. Corso, S. de Gironcoli, S. Fabris, G. Fratesi, R. Gebauer, U. Gerstmann, C. Gougoussis, A. Kokalj, M. Lazzeri, L. Martin-Samos, N. Marzari, F. Mauri, R. Mazzarello, S. Paolini, A. Pasquarello, L. Paulatto, C. Sbraccia, S. Scandolo, G. Sclauzero, A. P. Seitsonen, A. Smogunov, P. Umari, and R. M. Wentzcovitch, J. Phys.: Condensed Matter **21**, 395502 (19pp) (2009).
[44] J. P. Perdew, K. Burke, and M. Ernzerhof, Phys. Rev. Lett. **77**, 3865 (1996).
[45] D. Vanderbilt, Phys. Rev. B **41**, 7892 (1990).
[46] N. Troullier and J. L. Martins, Phys. Rev. B **43**, 1993 (1991).
[47] H. J. Monkhorst and J. D. Pack, Phys. Rev. B **13**, 5188 (1976).
[48] M. Methfessel and A. T. Paxton, Phys. Rev. B **40**, 3616 (1989).
[49] U. Burkhardt, V. Gurin, F. Haarmann, H. Borrmann, W. Schnelle, A. Yaresko, and Y. Grin, J. Solid State Chemistry **177**, 389 (2004).
[50] S. Margadonna, K. Prassides, I. Arvanitidis, M. Pissas, G. Papavassiliou, and A. N. Fitch, Phys. Rev. B **66**, 014518 (2002).
[51] P. Giannozzi, S. de Gironcoli, P. Pavone, and S. Baroni, Phys. Rev. B **43**, 7231 (1991).
[52] B. Grabowski, L. Ismer, T. Hickel, and J. Neugebauer, Phys. Rev. B **79**, 134106 (2009).